

Short Communication

# Synthesis and Electrochemical Properties of Intermediate Temperature SrCe<sub>0.6</sub>Zr<sub>0.3</sub>Er<sub>0.1</sub>O<sub>3-α</sub>-molten Carbonate Composite Electrolyte

Wenli Hu<sup>1</sup>, Wei Chen<sup>1</sup>, Hongtao Wang<sup>1,2\*</sup>

<sup>1</sup> Fuyang Preschool Education College, Fuyang 236015, China

<sup>2</sup> School of Chemical and Material Engineering, Fuyang Normal University, Fuyang 236037, China

\*E-mail: [hongtaoking3@163.com](mailto:hongtaoking3@163.com)

Received: 5 January 2019 / Accepted: 10 February 2019 / Published: 10 March 2019

An erbium-doped SrCeO<sub>3</sub>/SrZrO<sub>3</sub> electrolyte was synthesized via a sol-gel method using zirconium nitrate, cerium nitrate, strontium nitrate, nitric acid, citric acid and erbium oxide as raw materials. And SrCe<sub>0.6</sub>Zr<sub>0.3</sub>Er<sub>0.1</sub>O<sub>3-α</sub>-molten carbonate composite electrolyte was obtained at a low synthesis temperature. The thermal gravimetry analysis-differential scanning calorimetry (TGA-DSC) was tested to determine the formation temperature of SrCeO<sub>3</sub>/SrZrO<sub>3</sub> solid solution phase. The structure (X-ray diffractometer, XRD), morphology (scanning electron microscope, SEM), conductivities and H<sub>2</sub>/O<sub>2</sub> fuel cells of SrCe<sub>0.6</sub>Zr<sub>0.3</sub>Er<sub>0.1</sub>O<sub>3-α</sub> and SrCe<sub>0.6</sub>Zr<sub>0.3</sub>Er<sub>0.1</sub>O<sub>3-α</sub>-Na<sub>2</sub>CO<sub>3</sub>-Li<sub>2</sub>CO<sub>3</sub> were studied at 400-600 °C. The highest power densities of SrCe<sub>0.6</sub>Zr<sub>0.3</sub>Er<sub>0.1</sub>O<sub>3-α</sub> and SrCe<sub>0.6</sub>Zr<sub>0.3</sub>Er<sub>0.1</sub>O<sub>3-α</sub>-Na<sub>2</sub>CO<sub>3</sub>-Li<sub>2</sub>CO<sub>3</sub> were 16.3 mW·cm<sup>-2</sup> and 247.5 mW·cm<sup>-2</sup> at 600 °C, respectively.

**Keywords:** Composite; SrCeO<sub>3</sub>; Electrolyte; Conductivity; Fuel cell

## 1. INTRODUCTION

Inorganic SrCeO<sub>3</sub>-based solid electrolytes have excellent protonic conduction in water-saturated hydrogen atmospheres at 600-1000 °C. They are extensively used in fuel cells, solid sensors, organic reactors and hydrogen pumps etc. [1–10]. Normally, Ce<sup>4+</sup> was doped with the trivalent elements such as Y<sup>3+</sup>, Eu<sup>3+</sup>, Yb<sup>3+</sup> and Tm<sup>3+</sup> can improve the conductivities of SrCeO<sub>3</sub> [11–16]. Tsuji et al. synthesized SrCe<sub>0.9</sub>Eu<sub>0.1</sub>O<sub>3-α</sub> by using the solid-state reaction after calcining at 1550 °C for 10 h, respectively [11]. Li et al. studied an SrCe<sub>0.9</sub>Eu<sub>0.1</sub>O<sub>3-α</sub> protonic solid electrolytes to assemble a organic reactor for H<sub>2</sub> production [12]. However, the chemical stabilities of SrCeO<sub>3</sub>-based solid electrolytes are poor. In contrast, SrZrO<sub>3</sub>-based solid electrolytes are stable. Therefore, SrCeO<sub>3</sub>/SrZrO<sub>3</sub> solid solutions

which have high chemical stabilities and conductivities were investigated [13–16]. For example, Bredesen et al. [13] studied thulium or ytterbium doped SrCeO<sub>3</sub>/SrZrO<sub>3</sub> solid solution which applied to hydrogen permeability. The electro-negativity and the ionic radii of Er<sup>3+</sup> are 1.24 and 0.89 Å, which are much closer in electro-negativity and ionic radius to Y<sup>3+</sup> (1.22, 0.90 Å), Yb<sup>3+</sup> (1.3, 0.87 Å) and Tm<sup>3+</sup> (1.25, 0.88 Å). In our opinion, if these trivalent elements have almost the same electro-negativity and ionic radius, it is logical to assume that the Er<sup>3+</sup>-doped SrCeO<sub>3</sub> should also exhibit high proton conductivity. Therefore, erbium-doped SrCeO<sub>3</sub>/SrZrO<sub>3</sub> is the object in the study.

Over the past decade, composite electrolytes such as BaCeO<sub>3</sub>, LaGaO<sub>3</sub>, CeO<sub>2</sub>-based solid ceramic-carbonates, have been extensively investigated for intermediate temperature (400–600 °C) fuel cells [17–23]. Wang et al. synthesized a La<sub>0.9</sub>Sr<sub>0.1</sub>Ga<sub>0.8</sub>Mg<sub>0.2</sub>O<sub>2.85</sub>-(Li/Na)<sub>2</sub>CO<sub>3</sub> and it had a stable conductivity of 7-9×10<sup>-2</sup> S·cm<sup>-1</sup> at 600 °C [20]. Marques et al. found that the conductivities of Ce<sub>0.5</sub>Yb<sub>0.5</sub>O<sub>1.75</sub>-Li<sub>2</sub>CO<sub>3</sub>-Na<sub>2</sub>CO<sub>3</sub> composite electrolyte exceeded 0.1 S·cm<sup>-1</sup> above 500 °C [22]. Our previous studies have shown that SrCeO<sub>3</sub>-NaCl-KCl composite electrolytes had excellent intermediate temperature electrochemical properties [24–25]. However, there are few studies about SrCeO<sub>3</sub>/SrZrO<sub>3</sub> solid solution-carbonate composite electrolytes.

In this study, an erbium-doped SrCeO<sub>3</sub>/SrZrO<sub>3</sub> electrolyte was synthesized via a sol-gel method. And SrCe<sub>0.6</sub>Zr<sub>0.3</sub>Er<sub>0.1</sub>O<sub>3-α</sub>-molten carbonate composite electrolyte was obtained at a low temperature. The structure (XRD), morphology (SEM), conductivities and H<sub>2</sub>/O<sub>2</sub> fuel cells of SrCe<sub>0.6</sub>Zr<sub>0.3</sub>Er<sub>0.1</sub>O<sub>3-α</sub> and SrCe<sub>0.6</sub>Zr<sub>0.3</sub>Er<sub>0.1</sub>O<sub>3-α</sub>-Na<sub>2</sub>CO<sub>3</sub>-Li<sub>2</sub>CO<sub>3</sub> were studied at 400-600 °C.

## 2. EXPERIMENTAL

SrCe<sub>0.6</sub>Zr<sub>0.3</sub>Er<sub>0.1</sub>O<sub>3-α</sub> was synthesized via a sol-gel method using zirconium nitrate, cerium nitrate, strontium nitrate, nitric acid, citric acid and erbium oxide as raw materials. Firstly, erbium oxide was dissolved in nitric acid and zirconium nitrate, cerium nitrate and strontium nitrate were mixed in distilled water. Then, the pH was adjusted to 8-9 with an ammonia solution using citric acid as complexing agent. Finally, SrCe<sub>0.6</sub>Zr<sub>0.3</sub>Er<sub>0.1</sub>O<sub>3-α</sub> was prepared after being calcined at 1200 °C and 1540 °C for 5 h, respectively.

The molten carbonate salt (mole ratio of Li<sub>2</sub>CO<sub>3</sub>:Na<sub>2</sub>CO<sub>3</sub> =1:1) was obtained after being heated at 580 °C [26]. The mixtures (weight ratio of the molten carbonate salt and SrCe<sub>0.6</sub>Zr<sub>0.3</sub>Er<sub>0.1</sub>O<sub>3-α</sub> =1:4) were calcined at 620 °C for 1 h to synthesize SrCe<sub>0.6</sub>Zr<sub>0.3</sub>Er<sub>0.1</sub>O<sub>3-α</sub>-Na<sub>2</sub>CO<sub>3</sub>-Li<sub>2</sub>CO<sub>3</sub>.

TGA-DSC was tested using the SrCe<sub>0.6</sub>Zr<sub>0.3</sub>Er<sub>0.1</sub>O<sub>3-α</sub> precursor in nitrogen from 25 °C to 1000 °C with a heating rate of 15 °C·min<sup>-1</sup>. The electrolyte structures and morphologies of SrCe<sub>0.6</sub>Zr<sub>0.3</sub>Er<sub>0.1</sub>O<sub>3-α</sub> and SrCe<sub>0.6</sub>Zr<sub>0.3</sub>Er<sub>0.1</sub>O<sub>3-α</sub>-Na<sub>2</sub>CO<sub>3</sub>-Li<sub>2</sub>CO<sub>3</sub> were measured using XRD and SEM. For conductivities measurements, SrCe<sub>0.6</sub>Zr<sub>0.3</sub>Er<sub>0.1</sub>O<sub>3-α</sub>-Na<sub>2</sub>CO<sub>3</sub>-Li<sub>2</sub>CO<sub>3</sub> and SrCe<sub>0.6</sub>Zr<sub>0.3</sub>Er<sub>0.1</sub>O<sub>3-α</sub> were processed into thin wafers (electrode area = 0.50 cm<sup>2</sup>, thickness = 1.0-1.1 mm). The resistance values were obtained using an electrochemical analyzer (CHI660E, made in China) in the frequency range of 1 Hz–1 MHz from 400 °C to 600 °C in air. H<sub>2</sub>/O<sub>2</sub> fuel cells were also tested using SrCe<sub>0.6</sub>Zr<sub>0.3</sub>Er<sub>0.1</sub>O<sub>3-α</sub>-Na<sub>2</sub>CO<sub>3</sub>-Li<sub>2</sub>CO<sub>3</sub> and SrCe<sub>0.6</sub>Zr<sub>0.3</sub>Er<sub>0.1</sub>O<sub>3-α</sub> as electrolyte at 600 °C.

### 3. RESULTS AND DISCUSSION

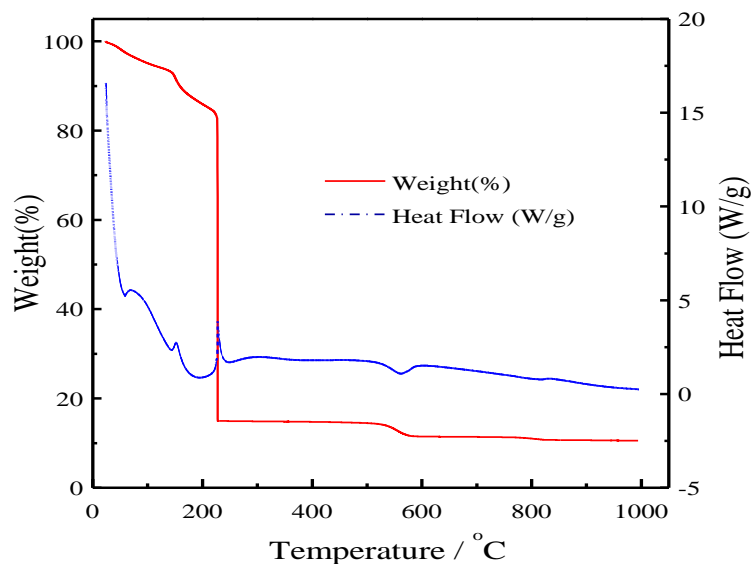


**Figure 1.** TGA-DSC plot of the  $\text{SrCe}_{0.6}\text{Zr}_{0.3}\text{Er}_{0.1}\text{O}_{3-\alpha}$  precursor.

The TGA-DSC curve of the  $\text{SrCe}_{0.6}\text{Zr}_{0.3}\text{Er}_{0.1}\text{O}_{3-\alpha}$  precursor is shown in Fig. 1. The plot shows a 16.5% weight loss from 25 °C to 225 °C which is attributed to the evaporation of water and ammonia from the dry gel. There was a severe weight loss accompanied by an exothermic peak in a very narrow temperature range from 225 to 230 °C which is ascribed to the decomposition of ammonium salt and citric acid. A gentle declining weight loss was found from 530 to 580 °C which is attributed to the incomplete nitrate [27–28]. TGA and DSC plots are almost horizontal after 980 °C which means that the temperature is close to the formation of  $\text{SrCeO}_3/\text{SrZrO}_3$  solid solution phase. Therefore, the first calcined temperature is 1200 °C.

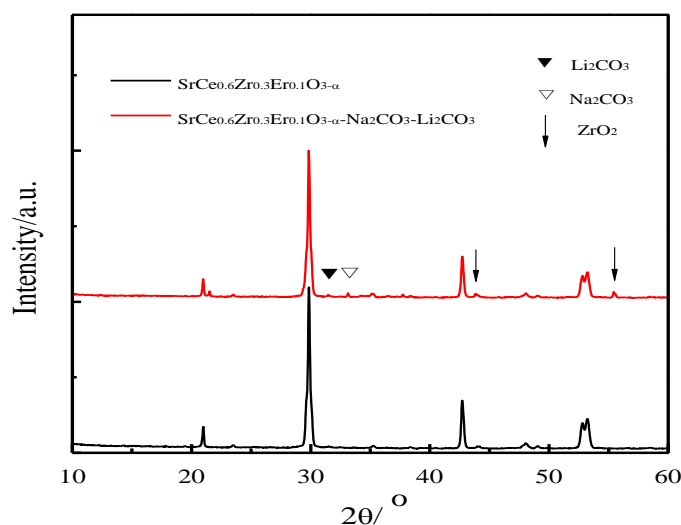


**Figure 2.** XRD patterns of  $\text{SrCe}_{0.6}\text{Zr}_{0.3}\text{Er}_{0.1}\text{O}_{3-\alpha}$  and  $\text{SrCe}_{0.6}\text{Zr}_{0.3}\text{Er}_{0.1}\text{O}_{3-\alpha}\text{-Na}_2\text{CO}_3\text{-Li}_2\text{CO}_3$ .

The XRD patterns of  $\text{SrCe}_{0.6}\text{Zr}_{0.3}\text{Er}_{0.1}\text{O}_{3-\alpha}$  and  $\text{SrCe}_{0.6}\text{Zr}_{0.3}\text{Er}_{0.1}\text{O}_{3-\alpha}\text{-Na}_2\text{CO}_3\text{-Li}_2\text{CO}_3$  are shown in Fig. 2. The diffraction peaks confirm that  $\text{SrCe}_{0.6}\text{Zr}_{0.3}\text{Er}_{0.1}\text{O}_{3-\alpha}$  is consistent with the standard  $\text{SrCeO}_3$  crystal plane. There are diffraction peaks of  $\text{Li}_2\text{CO}_3$ ,  $\text{Na}_2\text{CO}_3$  and  $\text{ZrO}_2$  besides  $\text{SrCeO}_3$  phase in the  $\text{SrCe}_{0.6}\text{Zr}_{0.3}\text{Er}_{0.1}\text{O}_{3-\alpha}\text{-Na}_2\text{CO}_3\text{-Li}_2\text{CO}_3$  pattern.

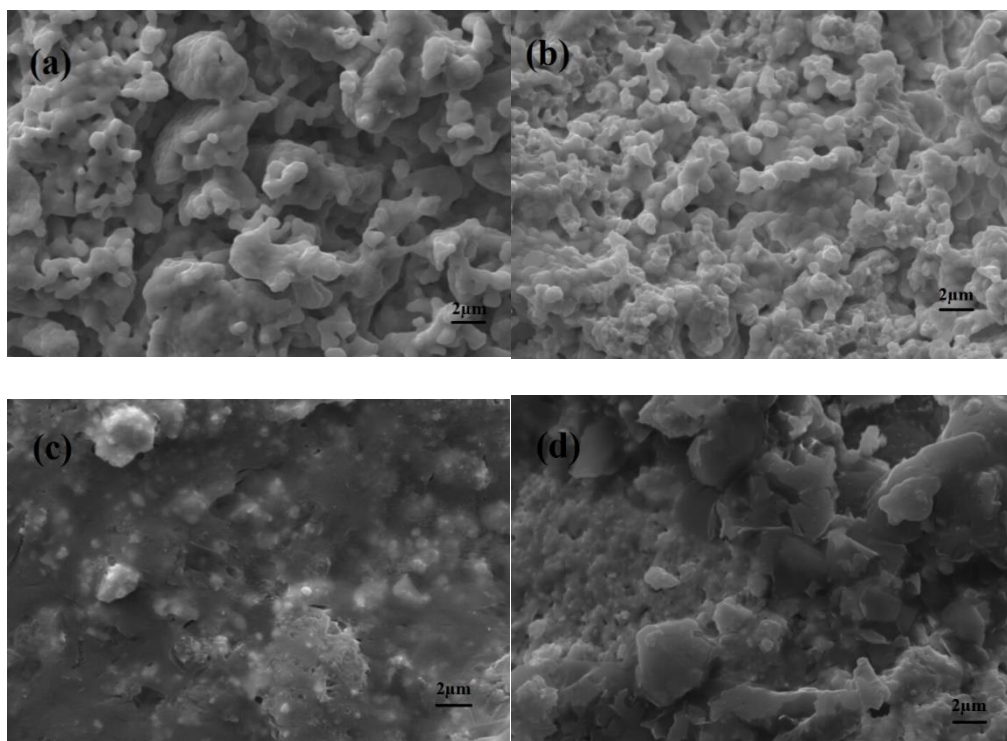


**Figure 3.** (a,b) SEM photos of  $\text{SrCe}_{0.6}\text{Zr}_{0.3}\text{Er}_{0.1}\text{O}_{3-\alpha}$  pellet calcined at 1540 °C for 5 h; (c,d) external and cross-sectional surfaces of  $\text{SrCe}_{0.6}\text{Zr}_{0.3}\text{Er}_{0.1}\text{O}_{3-\alpha}\text{-Na}_2\text{CO}_3\text{-Li}_2\text{CO}_3$ .

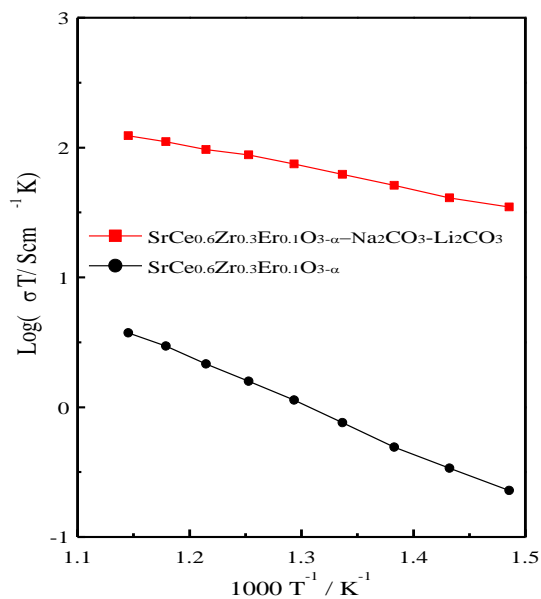


**Figure 4.** The  $\log(\sigma T) \sim 1000 T^{-1}$  plots of  $\text{SrCe}_{0.6}\text{Zr}_{0.3}\text{Er}_{0.1}\text{O}_{3-\alpha}$  and  $\text{SrCe}_{0.6}\text{Zr}_{0.3}\text{Er}_{0.1}\text{O}_{3-\alpha}\text{-Na}_2\text{CO}_3\text{-Li}_2\text{CO}_3$  in air from 400 °C to 600 °C.

The result illustrates that  $\text{Na}_2\text{CO}_3\text{-Li}_2\text{CO}_3$  melts entry into  $\text{SrCeO}_3/\text{SrZrO}_3$  solid solution to reduce the limitation of  $\text{ZrO}_2$ . Marques et al. revealed that the introduction of  $\text{Li}_2\text{CO}_3\text{-Na}_2\text{CO}_3$  promoted a slight decomposition of  $\text{Ce}_{0.5}\text{Yb}_{0.5}\text{O}_{1.75}$  [22]. And combined with previous studies [22, 23, 29],  $\text{Na}_2\text{CO}_3\text{-Li}_2\text{CO}_3$  coexists in two forms of crystalline and amorphous phases in  $\text{SrCe}_{0.6}\text{Zr}_{0.3}\text{Er}_{0.1}\text{O}_{3-\alpha}\text{-Na}_2\text{CO}_3\text{-Li}_2\text{CO}_3$ .

The SEM photos of  $\text{SrCe}_{0.6}\text{Zr}_{0.3}\text{Er}_{0.1}\text{O}_{3-\alpha}$  (a,b) and  $\text{SrCe}_{0.6}\text{Zr}_{0.3}\text{Er}_{0.1}\text{O}_{3-\alpha}\text{-Na}_2\text{CO}_3\text{-Li}_2\text{CO}_3$  (c,d) are shown in Fig. 3. From Fig. 3(a,b), the sintered  $\text{SrCe}_{0.6}\text{Zr}_{0.3}\text{Er}_{0.1}\text{O}_{3-\alpha}$  has clear agglomeration with a grain size is 2-6  $\mu\text{m}$ . From Fig. 3(c,d), there is an interlacing composition between  $\text{SrCe}_{0.6}\text{Zr}_{0.3}\text{Er}_{0.1}\text{O}_{3-\alpha}$  and  $\text{Li}_2\text{CO}_3\text{-Na}_2\text{CO}_3$ . It can be observed that the  $\text{SrCe}_{0.6}\text{Zr}_{0.3}\text{Er}_{0.1}\text{O}_{3-\alpha}$  particles are nestled inside molten carbonate salt which makes the composite electrolyte into a continuous 3-D reticulated structure [17].

Fig. 4 shows the  $\log(\sigma T) \sim 1000 T^{-1}$  plots of  $\text{SrCe}_{0.6}\text{Zr}_{0.3}\text{Er}_{0.1}\text{O}_{3-\alpha}$  and  $\text{SrCe}_{0.6}\text{Zr}_{0.3}\text{Er}_{0.1}\text{O}_{3-\alpha}\text{-Na}_2\text{CO}_3\text{-Li}_2\text{CO}_3$  in air from 400  $^\circ\text{C}$  to 600  $^\circ\text{C}$ . From Fig. 4, the slope of  $\text{SrCe}_{0.6}\text{Zr}_{0.3}\text{Er}_{0.1}\text{O}_{3-\alpha}\text{-Na}_2\text{CO}_3\text{-Li}_2\text{CO}_3$  is lower than that of  $\text{SrCe}_{0.6}\text{Zr}_{0.3}\text{Er}_{0.1}\text{O}_{3-\alpha}$  which means the conduction ion migration ability of the former is strong. The activation energies of  $\text{SrCe}_{0.6}\text{Zr}_{0.3}\text{Er}_{0.1}\text{O}_{3-\alpha}$  and  $\text{SrCe}_{0.6}\text{Zr}_{0.3}\text{Er}_{0.1}\text{O}_{3-\alpha}\text{-Na}_2\text{CO}_3\text{-Li}_2\text{CO}_3$  are  $31.6 \pm 0.7 \text{ kJ}\cdot\text{mol}^{-1}$  and  $69.8 \pm 0.8 \text{ kJ}\cdot\text{mol}^{-1}$ , respectively. The conductivities of  $\text{SrCe}_{0.6}\text{Zr}_{0.3}\text{Er}_{0.1}\text{O}_{3-\alpha}$  and  $\text{SrCe}_{0.6}\text{Zr}_{0.3}\text{Er}_{0.1}\text{O}_{3-\alpha}\text{-Na}_2\text{CO}_3\text{-Li}_2\text{CO}_3$  vary from  $3.4 \times 10^{-4} \text{ S}\cdot\text{cm}^{-1}$  to  $4.1 \times 10^{-3} \text{ S}\cdot\text{cm}^{-1}$  and  $5.2 \times 10^{-2} \text{ S}\cdot\text{cm}^{-1}$  to  $1.4 \times 10^{-1} \text{ S}\cdot\text{cm}^{-1}$  at 400–600  $^\circ\text{C}$ , correspondingly. The lower activation energy and higher conductivities of  $\text{SrCe}_{0.6}\text{Zr}_{0.3}\text{Er}_{0.1}\text{O}_{3-\alpha}\text{-Na}_2\text{CO}_3\text{-Li}_2\text{CO}_3$  indicate that the molten carbonate salt provide an additional transport function between the interfaces [17,23,30].

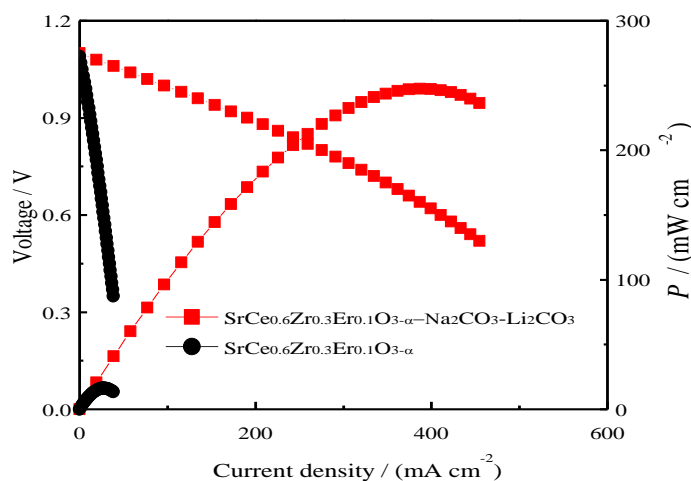


**Figure 5.** The  $I$ - $V$ - $P$  curves of  $\text{SrCe}_{0.6}\text{Zr}_{0.3}\text{Er}_{0.1}\text{O}_{3-\alpha}$  and  $\text{SrCe}_{0.6}\text{Zr}_{0.3}\text{Er}_{0.1}\text{O}_{3-\alpha}\text{-Na}_2\text{CO}_3\text{-Li}_2\text{CO}_3$  at 600  $^\circ\text{C}$ .

**Table 1.** The highest power densities of SrCe<sub>0.6</sub>Zr<sub>0.3</sub>Er<sub>0.1</sub>O<sub>3-α</sub>-Na<sub>2</sub>CO<sub>3</sub>-Li<sub>2</sub>CO<sub>3</sub> and similar electrolytes in the literatures.

Electrolytes	Highest power densities
SrCe <sub>0.6</sub> Zr <sub>0.3</sub> Er <sub>0.1</sub> O <sub>3-α</sub> -Na <sub>2</sub> CO <sub>3</sub> -Li <sub>2</sub> CO <sub>3</sub> (80: 20)	247.5 mW·cm <sup>-2</sup> , 600 °C, in this work
Ce <sub>0.8</sub> Sm <sub>0.2</sub> O <sub>1.9</sub> - (Li/Na) <sub>2</sub> CO <sub>3</sub> (80: 20)	605 mW·cm <sup>-2</sup> , 575 °C, [31]
Ce <sub>0.8</sub> Sm <sub>0.2</sub> O <sub>1.9</sub> - (Li/Na) <sub>2</sub> CO <sub>3</sub> (60: 40)	240 mW·cm <sup>-2</sup> , 575 °C, [31]
Ce <sub>0.9</sub> Gd <sub>0.1</sub> O <sub>1.95</sub> - LiCl-SrCl <sub>2</sub> (12: 5)	245 mW·cm <sup>-2</sup> , 550 °C, 320 mW·cm <sup>-2</sup> , 590 °C, [18]

Fig. 5 shows the *I-V-P* curves of SrCe<sub>0.6</sub>Zr<sub>0.3</sub>Er<sub>0.1</sub>O<sub>3-α</sub> and SrCe<sub>0.6</sub>Zr<sub>0.3</sub>Er<sub>0.1</sub>O<sub>3-α</sub>-Na<sub>2</sub>CO<sub>3</sub>-Li<sub>2</sub>CO<sub>3</sub> at 600 °C. The highest power density obtained with using SrCe<sub>0.6</sub>Zr<sub>0.3</sub>Er<sub>0.1</sub>O<sub>3-α</sub>-Na<sub>2</sub>CO<sub>3</sub>-Li<sub>2</sub>CO<sub>3</sub> as the electrolyte is 247.5 mW·cm<sup>-2</sup>, which was estimated to be about 15 times higher than that of the SrCe<sub>0.6</sub>Zr<sub>0.3</sub>Er<sub>0.1</sub>O<sub>3-α</sub> with 16.3 mW·cm<sup>-2</sup>. This may be attributed to the homogeneous 3-D reticulated structure of the composite electrolyte. The *P<sub>h</sub>* value of our result is close to the fuel cell performance of 60 wt% Ce<sub>0.8</sub>Sm<sub>0.2</sub>O<sub>1.9</sub>-40 wt% (Li/Na)<sub>2</sub>CO<sub>3</sub> (575 °C) and Ce<sub>0.9</sub>Gd<sub>0.1</sub>O<sub>1.95</sub>- LiCl-SrCl<sub>2</sub> (550 °C), however, lower than 80 wt% Ce<sub>0.8</sub>Sm<sub>0.2</sub>O<sub>1.9</sub>-20 wt% (Li/Na)<sub>2</sub>CO<sub>3</sub> (575 °C) and Ce<sub>0.9</sub>Gd<sub>0.1</sub>O<sub>1.95</sub>- LiCl-SrCl<sub>2</sub> (590 °C) as shown in Table 1 [18, 31]. This may be due to the different electrolyte types and fuel cell construction.

#### 4. CONCLUSIONS

An erbium-doped SrCeO<sub>3</sub>/SrZrO<sub>3</sub> electrolyte was synthesized via a sol-gel method and SrCe<sub>0.6</sub>Zr<sub>0.3</sub>Er<sub>0.1</sub>O<sub>3-α</sub>-molten carbonate composite electrolyte was obtained at a low synthesis temperature. The XRD patterns indicate that Na<sub>2</sub>CO<sub>3</sub>-Li<sub>2</sub>CO<sub>3</sub> coexists in two forms of crystalline and amorphous phases in SrCe<sub>0.6</sub>Zr<sub>0.3</sub>Er<sub>0.1</sub>O<sub>3-α</sub>-Na<sub>2</sub>CO<sub>3</sub>-Li<sub>2</sub>CO<sub>3</sub>. The SEM photos show that the SrCe<sub>0.6</sub>Zr<sub>0.3</sub>Er<sub>0.1</sub>O<sub>3-α</sub> particles are nestled inside molten carbonate salt to form a continuous 3-D reticulated structure. The highest power density and conductivity of SrCe<sub>0.6</sub>Zr<sub>0.3</sub>Er<sub>0.1</sub>O<sub>3-α</sub>-Na<sub>2</sub>CO<sub>3</sub>-Li<sub>2</sub>CO<sub>3</sub> are 247.5 mW·cm<sup>-2</sup> and 1.4×10<sup>-1</sup> S·cm<sup>-1</sup> at 600 °C, respectively.

#### ACKNOWLEDGEMENTS

This work was supported by the National Natural Science Foundation (No. 51402052) of China, The Natural Science Project of Anhui Province (No. KJ2018A0337, KJ2018A0980), Excellent Youth Foundation of Anhui Educational Committee (No. gxyq2018046), Horizontal cooperation project of Fuyang municipal government and Fuyang Normal College (No. XDHX2016019, XDHXTD201704).

#### References

1. C. Bernuy-Lopez, L. Rioja-Monllor, T. Nakamura, S. Ricote, R. O'Hayre, K. Amezawa, M. Einarsrud and T. Grande, *Materials*, 11 (2018) 196.

2. G. L. Liu, W. Liu Q. Kou and S. J. Xiao, *Int. J. Electrochem. Sci.*, 13 (2018) 2641.
3. D.-K. Lim, J.-H. Kim, A.U. Chavan, T.-R. Lee, Y.-S. Yoo and S.-J. Song, *Ceram. Int.*, 42 (2016) 3776.
4. T.S. Li, M. Xu, C. Gao, B. Wang, X. Liu, B. Li and W.G. Wang, *J. Power Sources*, 258 (2014) 1.
5. Y. N. Chen, T. Tian, Z. H. Wan, F. Wu, J. T. Tan and M. Pan, *Int. J. Electrochem. Sci.*, 13 (2018) 3827.
6. Y. Wan, B. He, R. Wang, Y. Ling and L. Zhao, *J. Power Sources*, 347 (2017) 14.
7. S. Pang, Y. Su, G. Yang, X. Shen, M. Zhu, X. Wu, S. Li, X. Yang and X. Xi, *Ceram. Int.*, 44 (2018) 21902.
8. J. Luo, A.H. Jensen, N.R. Brooks, J. Sniekers, M. Knipper, D. Aili, Q. Li, B. Vanroy, M. Wübbenhorst, F. Yan, L.V. Meervelt, Z. Shao, J. Fang, Z.-H. Luo, D.E.D. Vos, K. Binnemans and J. Fransaer, *Energy Environ. Sci.*, 8 (2015) 1276.
9. Raghvendra and P. Singh, *Ceram. Int.*, 43 (2017) 11692.
10. K. Leonard, Y.-S. Lee, Y. Okuyama, K. Miyazaki and H. Matsumoto, *Int. J. Hydrogen. Energ.*, 42 (2017) 3926.
11. T. Tsuji and T. Nagano, *Solid State Ionics*, 136-137(2000)179.
12. J. Li, H. Yoon, T. Oh and E.D. Wachsman, *Appl. Catal. B: Environ.*, 92 (2009) 234.
13. W. Xing, P.I. Dahl, L.V. Roaas, M.-L. Fontaine, Y. Larring, P.P. Henriksen and R. Bredesen, *J. Membrane Sci.*, 473(2015)327.
14. I.-M. Hung, Y.-J. Chiang, J. S.-C. Jang, J.-C. Lin, S.-W. Lee, J.-K. Chang and C.-S. His, *J. Eur. Ceram. Soc.*, 35 (2015) 163.
15. Y. Okuyama, K. Isa, Y.S. Lee, T. Sakai and H. Matsumoto, *Solid State Ionics*, 275 (2015) 35.
16. P.S. Mahadik, D. Jain, A.N. Shirsat, N. Manoj, S. Varma, B.N. Wani and S.R. Bharadwaj, *Electrochim. Acta*, 219 (2016) 614.
17. Y. Hei, J. Huang, C. Wang and Z. Mao, *Int. J. Hydrogen Energ.*, 39 (2014) 14328.
18. Q.X. Fu, S.W. Zha, W. Zhang, D.K. Peng, G.Y. Meng and B. Zhu, *J. Power Sources*, 104 (2002) 73.
19. C. Slim, L. Baklouti, M. Cassir and A. Ringuedé, *Electrochim. Acta*, 123 (2014) 127.
20. F. Xie, C. Wang, Z. Mao and Z. Zhan, *Int. J. Hydrogen Energ.*, 39 (2014) 14397.
21. A.K. Ojha, V. Ponnillavan and S. Kannan, *Ceram. Int.*, 43 (2017) 686.
22. N.C.T. Martins, S. Rajesh and F.M.B. Marques, *Mater. Res. Bull.*, 70 (2015) 449.
23. J.T. Kim, T.H. Lee, K.Y. Park, Y. Seo, K.B. Kim, S.J. Song, B. Park and J.Y. Park, *J. Power Sources*, 275 (2015) 563.
24. R. Shi, W. Chen, W. Hu, J. Liu and H. Wang, *Materials*, 11 (2018) 1583.
25. L. Sun, H. Miao and H. Wang, *Solid State Ionics*, 311 (2017) 41.
26. X. Liu, N. Fechler and M. Antonietti, *Chem. Soc. Rev.*, 42 (2013) 8237.
27. A. Matsuda, S. Oh, V.H. Nguyen, Y. Daiko, G. Kawamura and H. Muto, *Electrochim. Acta*, 56 (2011) 9364.
28. M.T. Soo, N. Prastomo, A. Matsuda, G. Kawamura, H. Muto, A.F.M. Noor, Z. Lockman and K.Y. Cheong, *Appl. Surf. Sci.*, 258 (2012) 5250.
29. S. Shawuti and M. A. Gulgun, *J. Power Sources*, 267 (2014) 128.
30. X. Li, N. Xu, L. Zhang and K. Huang, *Electrochem. Commun.*, 13 (2011) 694.
31. M. Chen, H. Zhang, L. Fan, C. Wang and B. Zhu, *Int. J. Hydrogen Energ.*, 39 (2014) 12309.